




Numerical Simulation of Soret and Dufour Effects on Micropolar Nanofluid Flow with Swimming Gyrotactic Microorganisms

Keshab Borah ¹ , Jadav Konch ^{2,*} , Shyamanta Chakraborty ³ 

¹ Department of Mathematics, Gauhati University, Assam, India; keshabborah388@gmail.com;

² Department of Mathematics, Dhemaji College, Assam, 787057, India; jadavkonch@gmail.com;

³ UGC-MMTTC, Gauhati University, Guwahati, Assam, India; schakrabortyhrdc@gauhati.ac.in;

* Correspondence: jadavkonch@gmail.com;

Scopus Author ID 57148418700

Received: 14.05.2024; Accepted: 6.10.2024; Published: 14.02.2025

Abstract: The study numerically investigates the impacts of the Soret and Dufour effect under the influence of a chemical reaction on the flow of gyrotactic microorganisms and micropolar nanofluid over a stretching/shrinking sheet with the impact of radiation and viscous dissipation in the presence of a uniform magnetic field and a heat source. The nonlinear partial differential equations representing the flow system are transformed into a system of nonlinear ordinary differential equations using suitable similarity transformations. This system is then solved numerically using the fourth-order Runge-Kutta method with a shooting technique. The influence of relevant parameters on the velocity profile, microrotation profile, density profile of the motile microorganisms, temperature profile, and concentration profile is investigated and graphically represented. The study shows that an increase in Dufour and chemical reaction parameters leads to a proportional increase in temperature profile, while an inverse effect is observed in the concentration profiles with an increase in the aforementioned parameters. Furthermore, an increase in the Soret number significantly decreases both temperature and concentration profiles. The numerical values of heat transfer rate, mass transfer rate, and shear stress are determined for different values of the Soret, Dufour, and chemical reaction parameters, which are presented in tables and discussed.

Keywords: Soret number; Dufour number; micropolar nanofluid; radiation; chemical reaction; gyrotactic microorganisms.

© 2025 by the authors. This article is an open-access article distributed under the terms and conditions of the Creative Commons Attribution (CC BY) license (<https://creativecommons.org/licenses/by/4.0/>).

1. Introduction

The flow of fluids and the transfer of heat across a stretched surface are utilized in a variety of ways in engineering and related fields. The low thermal conductivity of convection fluids such as water, ethylene glycol, and oil leads to several difficulties developing electronic devices. To overcome this limitation and improve the thermal conductivity of convection fluids, several researchers have focussed on mixing nano- or micro-sized particles with their base fluids over the past decades. Mixing nanometre-sized particles with the base fluid is known as nanofluid and is used to improve the thermal conductivity of the mixed fluid.

Nanofluids have become increasingly important in recent years due to their wide range of applications, including in healthcare, the petroleum sector, and food processing. Many researchers are interested in convective heat transfer with nano-sized particle mixtures. In addition, nanoparticles increase the temperature of the so-called base fluid, which is the main

cause of heat transfer efficiency. To our knowledge, Choi and Eastman [1] were the first to propose the concept of nanofluid. They found that the addition of a few nanoparticles would increase thermal conductivity. Babu [2] mathematically investigated the unsteady MHD flow of a Casson nanofluid over an evolving vertical semi-infinite surface. Xie *et al.* [3] investigated the electrokinetic energy conversion for nanofluids in an MHD-based microtube. Ali *et al.* [4] investigated the effects of successive slips on the unsteady MHD flow of Maxwell nanofluids in the presence of a chemical reaction. Mohyud-Din *et al.* [5] investigated the dynamics of nanofluid flow over a moving flat plate. Their findings indicate that the heat conductivity improves with the number of nanoparticles. Akbari *et al.* [6] and Hayat *et al.* [7] investigated the same activity of nanoparticles. Kamal *et al.* [8] investigated the stability of MHD nanofluid flow over a stretching/shrinking plate in a stagnant point flow. Kumar *et al.* [9] investigated the flow of an unsteady MHD nanofluid through a slendering stretching plate. Mitra [10] investigated the computational modeling of the flow of a nanofluid through a heated inclined sheet. Chakraborty [11] investigated the nanofluid flow on an inclined porous plate. The flow of nanofluids through an inclined permeable surface with similar solutions was elaborated by Ziaei-Rad *et al.* [12]. The consequences of MHD non-Newtonian nanofluid flow through a nonlinear porous surface with sliding were studied by Raza *et al.* [13].

Mabood and Shateyi [14] conducted a study on the influence of multiple slip conditions on heat and mass transfer in transient hydro-magnetic flow, considering the effects of Soret and radiation. Das and Dorjee [15] investigated the MHD boundary layer motion of an incompressible fluid flowing over a moving vertical surface with a heat source. Kumar *et al.* [16] studied the MHD flow of a micropolar fluid over a stretching surface, considering viscous dissipation and the effects of Joule heating. Anwar *et al.* [17] investigated the MHD stagnation point flow of a micropolar nanofluid flowing over a stretched plate. Kumar *et al.* [18] analyzed the simultaneous effects of heat and mass transfer on a micropolar nanofluid's magnetohydrodynamic (MHD) flow over a stretching plate. Kumar *et al.* [19] discussed the physical aspects of the MHD flow of a micropolar fluid through an exponentially curved plate. Venkata *et al.* [20] demonstrated the heat and mass transport in MHD Casson nanofluid flow over an expanding sheet using thermophoresis and Brownian motion. Mabood *et al.* [21] further researched this by inserting nanoparticles to increase heat conductivity.

The mass flow process caused by a temperature gradient can be defined as thermodiffusion or the Soret effect. On the other hand, the Dufour effect can be characterized as a phenomenon of heat flow caused by a concentration gradient. In many heat transfer studies, the Soret and Dufour effects are ignored because they are considered lower-order effects than the other effects specified by Fourier's and Fick's laws. Sharada and Shankar [22] studied the effects of Soret/Dufour and thermal radiation with chemical reactions on Casson fluid when it flows over an exponentially expanding surface. Abdal *et al.* [23] studied a micropolar nanofluid's MHD mixed convective flow characteristics, considering radiation and heat source effects over a shrinking/stretching plate. More recently, Rehman *et al.* [24] studied the effects of buoyancy and radiation on micropolar nanofluid flowing over a stretching/shrinking sheet in the presence of a heat source.

Bioconvection is the collective movement of floating microorganisms that occurs due to spatial variations in fluid density in an area. The density differences in the liquid trigger this movement. The self-propulsion of microorganisms causes the surrounding liquid to move in a certain direction, creating a bioconvection flow. A microorganism is a living organism that is able to grow, multiply, respond to stimuli, and have a specific structure. Microorganisms are

extremely small and usually require a microscope for observation. Examples of microorganisms are algae, archaea, house dust mites, and bacteria. Ramzan *et al.* [25] investigated heat and mass transfer in a flow with gyrotactic microorganisms and nanoparticles. Ahmed *et al.* [26] investigated the effect of floating gyrotactic microorganisms and viscous dissipation on the flow of nanoparticles through a permeable medium. Hussain *et al.* [27] investigated a biomathematical model of magnetohydrodynamic nanofluid flow through a stretched cylinder. In this study, convective boundary conditions, Nield conditions, and the existence of gyrotactic floating microorganisms were considered. Researchers such as Shahid *et al.* [28], Waqas *et al.* [29], and Koriko *et al.* [30] have conducted important studies on motile gyrotactic microorganisms and nanofluids.

Motivated by the previous referenced works and several potential industrial applications, it is of utmost importance in this study to investigate the effects of Soret, Dufour, and chemical reaction on micropolar MHD nanofluid flow with floating gyrotactic microorganisms over a stretching plate. This paper will, therefore, extend the work of Rehman *et al.* [24] to investigate a more general problem involving the effects of Soret, Dufour, and chemical reaction on micropolar MHD nanofluid flow with floating gyrotactic microorganisms with a heat source. In addition, buoyancy and radiation effects are also considered. This study plots and tabulate the impacts of different flow parameters related to the governing equations. The problem is solved numerically using the fourth-order Runge-Kutta method, which is computationally more efficient.

2. Materials and Methods

This work investigates a steady two-dimensional magnetohydrodynamic(MHD) flow over a shrinking/stretching sheet with a heat source of an incompressible, electrically conducting micropolar nanofluid. It is hypothesized that the presence of nanoparticles and bioconvection do not change the direction or velocity of the microorganisms. The microorganisms exhibit a uniform shape, and their surface does not exhibit the formation of extracellular polymers. The x -axis runs along the plate, and the y -axis is perpendicular to it. The plate moves with velocity $U(x,t) = ax$, where a is the shrinkage/stretching rate along the x -axis. A transverse magnetic field $B(x) = B_0x^{-1/2}$ with $B_0 \neq 0$ is also applied, where B_0 is the strength of the magnetic field. The physical configuration of the flow is shown in Figure 1.

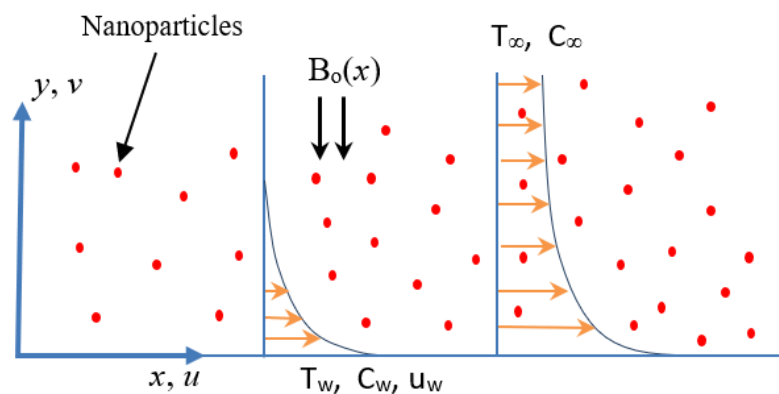


Figure 1. Physical configuration of the flow system.

Based on the above assumptions and following Rehman *et al.* [24], the equations that determine the flow are as follows:

$$\frac{\partial u}{\partial x} + \frac{\partial v}{\partial y} = 0 \tag{1}$$

$$u \frac{\partial u}{\partial x} + v \frac{\partial u}{\partial y} = \left(\frac{\mu+\kappa}{\rho}\right) \frac{\partial^2 u}{\partial y^2} + \frac{\kappa}{\rho} \frac{\partial N}{\partial y} - \frac{\sigma B^2 u}{\rho} + g\beta_T(T - T_\infty) + g\beta_C(C - C_\infty) \tag{2}$$

$$u \frac{\partial N}{\partial x} + v \frac{\partial N}{\partial y} = \frac{\gamma}{\rho j} \frac{\partial^2 N}{\partial y^2} - \frac{\kappa}{\rho j} \left(2N + \frac{\partial u}{\partial y}\right) \tag{3}$$

$$u \frac{\partial T}{\partial x} + v \frac{\partial T}{\partial y} = \alpha \left(1 + \frac{16 T_\infty^3 \sigma^*}{3k^* \kappa}\right) \frac{\partial^2 T}{\partial y^2} + Q'(T - T_\infty) + \tau \left(D_B \frac{\partial C}{\partial y} \frac{\partial T}{\partial y} + \frac{D_T}{T_\infty} \left(\frac{\partial T}{\partial y}\right)^2\right) + \left(\frac{\mu+\kappa}{\rho C_p}\right) \left(\frac{\partial u}{\partial y}\right)^2 + \frac{D_M K_T}{C_S C_p} \frac{\partial^2 C}{\partial y^2} \tag{4}$$

$$u \frac{\partial C}{\partial x} + v \frac{\partial C}{\partial y} = D_B \frac{\partial^2 C}{\partial y^2} + \frac{D_T}{T_\infty} \frac{\partial^2 T}{\partial y^2} - k_0(C - C_\infty) + \frac{D_M K_T}{T_M} \frac{\partial^2 T}{\partial y^2} \tag{5}$$

$$u \frac{\partial n}{\partial x} + v \frac{\partial n}{\partial y} + \frac{bW_C}{C_w - C_\infty} \left[\frac{\partial}{\partial y} \left(n \frac{\partial C}{\partial y}\right)\right] = D_n \frac{\partial^2 n}{\partial y^2} \tag{6}$$

The corresponding boundary conditions are:

$$\left. \begin{aligned} u = U(x, t), \quad v = v_w, \quad N = -m \frac{\partial u}{\partial y}, \quad T = T_w, \quad C = C_w, \quad n = n_w \quad \text{at } y = 0 \\ u \rightarrow 0, \quad N \rightarrow 0, \quad T \rightarrow T_\infty, \quad C \rightarrow C_\infty, \quad n \rightarrow n_\infty \quad \text{as } y \rightarrow \infty \end{aligned} \right\} \tag{7}$$

Where u and v denote the velocity components along the x and y axis respectively, μ stands for the coefficient of dynamic viscosity, κ for coefficient of vortex viscosity, ρ for the density of the fluid, N for the micro-rotational vector, $j = \frac{U}{a}$ for the micro-inertial density, $\gamma = \left(\mu + \frac{\kappa}{2}\right)j$ indicates the spin-gradient viscosity, σ the electrical conductivity, α the thermal diffusivity, g the gravitational acceleration, β_T the coefficient of thermal expansion, β_C the coefficient of expansion of the dissolved concentration, T the temperature of the solution, C the concentration of the solution, T_∞ is the ambient temperature, k^* is the mean absorption coefficient, C_∞ is the ambient concentration, σ^* is the Stefan-Boltzmann constant, k_0 is the chemical reaction rate constant, Q' is the constant heat source, D_B the Brownian diffusion coefficient, D_T is thermal diffusivity, C_p is the specific heat, C_s is the concentration susceptibility, D_M is the chemical molecular diffusivity, τ is the ratio between the effective heat capacity of the nanoparticles and the base fluid, D_n is the diffusivity of the microorganisms, n is the density of the motile microbes, bW_C is the swimming velocity of the cells.

To transform the partial differential equations governing the flow problem to ordinary differential equations, we employ the following standard similarity transformation:

$$\left. \begin{aligned} \eta = \sqrt{\frac{a}{v}} y, \quad f(\eta) = \frac{\psi}{x\sqrt{av}}, \quad g(\eta) = \sqrt{\frac{v}{a}} \frac{N}{ax}, \quad \theta(\eta) = \frac{T - T_\infty}{T_w - T_\infty} \\ \phi(\eta) = \frac{C - C_\infty}{C_w - C_\infty}, \quad \omega(\eta) = \frac{n - n_\infty}{n_w - n_\infty} \end{aligned} \right\} \tag{8}$$

The stream function ψ is defined as $u = \frac{\partial \psi}{\partial y}, v = -\frac{\partial \psi}{\partial x}$ which identically satisfied equation (1). Using the transformations represented by (8), equations (2) to (6) are transformed as under:

$$(1 + K)f''' - (f')^2 + ff'' + Kg' - Mf' + \lambda_1\theta + \lambda_2\phi = 0 \tag{9}$$

$$\left(1 + \frac{K}{2}\right)g'' + fg' - f'g - K(2g + f'') = 0 \tag{10}$$

$$\left(\frac{1+R_d}{Pr}\right)\theta'' + f\theta' + Q\theta + N_b\theta'\phi' + N_t(\theta')^2 + (1 + K)Ec(f'')^2 + Du\phi'' = 0 \tag{11}$$

$$\phi'' + Le f\phi' + \frac{N_t}{N_b}\theta'' - Kc Le\phi + Sc Le\theta'' = 0 \tag{12}$$

$$\omega'' + Sc_m f\omega' - Pe\xi\phi'' - Pe\omega\phi'' - Pe\phi'\omega' = 0 \tag{13}$$

The corresponding boundary conditions (7) become

$$\left. \begin{aligned} f(0) = F_A, f'(0) = 1, g(0) = -mf''(0), \theta(0) = 1, \phi(0) = 1, \omega(0) = 1 \text{ at } \eta = 0 \\ f'(\infty) = 0, g(\infty) = 0, \theta(\infty) = 0, \phi(\infty) = 0, \omega(\infty) = 0 \text{ as } \eta \rightarrow \infty \end{aligned} \right\} \tag{14}$$

The parameters in equations (9) to (13) are defined as

$$\begin{aligned} K = \frac{\kappa}{\mu}; M = \frac{\sigma B^2}{\rho a}; \lambda_1 = \frac{g\beta_T(T_w \rightarrow T_\infty)}{a^2 x}; \lambda_2 = \frac{g\beta_C(C_w \rightarrow C_\infty)}{a^2 x}; R_d = \frac{16 T_\infty^3 \sigma^*}{3k^* \kappa}; \\ Pe = \frac{bW_C}{D_n}; Pr = \frac{v}{\alpha}; \alpha = \frac{k}{\rho C_p}; Q = \frac{Q'}{a}; N_b = \frac{\tau D_B(C_w - C_\infty)}{v}; N_t = \frac{\tau D_T(T_w - T_\infty)}{v T_\infty}; \\ Kc = \frac{k_0}{a}; Ec = \frac{U^2}{C_p(T_w - T_\infty)}; Du = \frac{D_M K_T(C_w - C_\infty)}{v C_S C_p(T_w - T_\infty)}; Le = \frac{v}{D_B}; F_A = -\frac{v_w}{\sqrt{av}}; \\ Sr = \frac{D_M K_T(T_w - T_\infty)}{v T_M(C_w - C_\infty)}; Sc_m = \frac{v}{D_n} \end{aligned}$$

Where K is micropolar material parameter, M is magnetic parameter, R_d is radiation parameter, λ_1 and λ_2 are buoyancy parameters, Pr is Prandtl number, Q is heat source parameter, N_t represents thermophoresis parameter, N_b denotes the Brownian motion parameter, Ec represents the Eckert number, Du is Dufour number, Sr is Soret number, Le is the Lewis number, Kc is chemical reaction parameter, Sc_m is the Schmidt number for diffusing motile microorganisms, Pe is Peclet number, ξ is motile parameter, F_A is the injection/suction parameter.

2.1. Physical quantities of engineering interest.

In this problem, the skin friction coefficient (C_f), the Nusselt number (Nu), and the Sherwood number (Sh) are technically important physical quantities.

The skin friction at the plate can be calculated using the velocity field and is represented in non-dimensional form by

$$C_f = \frac{\tau_w}{\rho u_w^2}; \text{ where } \tau_w = \left[(\mu + \kappa) \frac{\partial u}{\partial y} + \kappa N \right]_{y=0} \tag{15}$$

That gives

$$\sqrt{Re} C_f = [1 + (1 - m)K] f''(0)$$

Here $Re = \frac{ax^2}{\nu}$ is the local Reynolds number.

The temperature field, in non-dimensional form, can be employed to determine the rate of heat transfer coefficient. The rate of heat transfer coefficient, which is stated in terms of the Nusselt number(Nu), can be found using the temperature field in non-dimensional form.

$$Nu = \frac{xq_w}{k(T_w - T_\infty)}, \text{ where } q_w = -k \left(\frac{\partial T}{\partial y} \right)_{y=0} \quad (16)$$

That gives $\frac{Nu}{\sqrt{Re}} = -\theta'(0)$

The mass transfer rate can be computed using the concentration field, which is given in non-dimensional form with regard to the Sherwood number(Sh).

$$Sh = \frac{j_w x}{D_B(C_w - C_\infty)}, \text{ where } j_w = -D_B \left(\frac{\partial C}{\partial y} \right)_{y=0} \quad (17)$$

That gives $\frac{Sh}{\sqrt{Re}} = -\phi'(0)$.

3. Results and Discussion

The nonlinear ordinary differential equations (9)-(13), subject to the boundary conditions (14), are solved numerically using the fourth-order Runge-Kutta shooting method. We have examined the influence of several key physical parameters, including K , Du , Kc , Sr , Sc_m , Pe , and Le on the motile microorganisms' density, velocity, angular velocity, temperature, and concentration profiles.

Figures 2–6 show the profiles of velocity, angular velocity, temperature, concentration, and motile microbe density profiles for different values of the material parameter (K). It can be seen from Figure 2 that the velocity profile increases with K . Physically, the material parameter is inversely correlated with the dynamic viscosity coefficient, so a larger number makes the fluid flow faster. Figure 3 shows that the angular velocity profile initially decreases with increasing values of K until it reaches the point $\eta \cong 1$, and after that, the angular velocity increases with K . As the material parameter increases, the micro-concentration of the liquid increases, which also changes the flow and increases the thickness of the boundary layer. Figures 4 and 5 show how increasing values of K leads to a decrease in fluid temperature and concentration. Figure 6 shows that the profile of the density of motile microbes decreases as the parameter K increases.

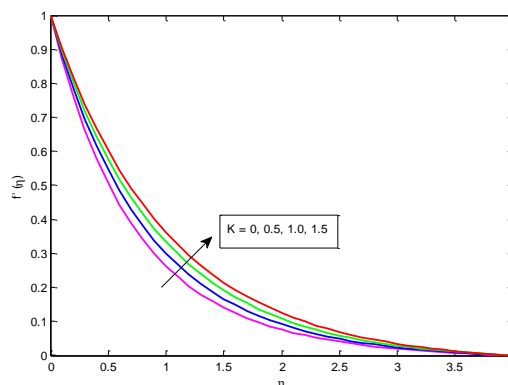


Figure 2. Effect of K on $f'(\eta)$.

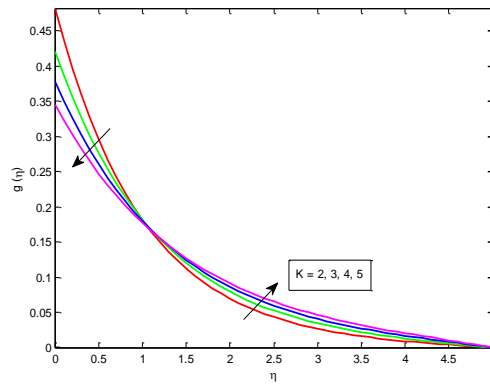


Figure 3. Effect of K on $g(\eta)$.

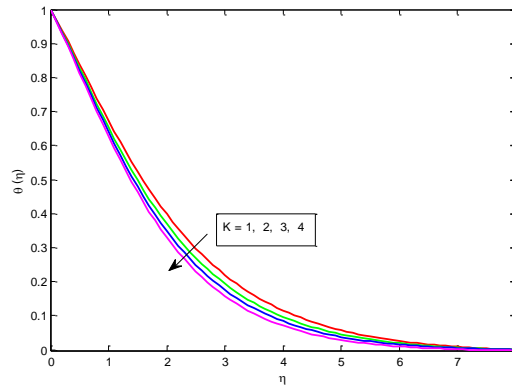


Figure 4. Effect of K on $\theta(\eta)$.

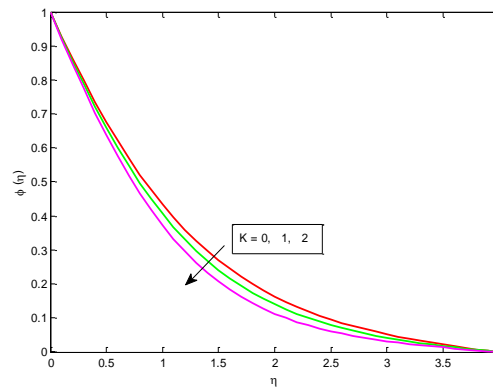


Figure 5. Effect of K on $\phi(\eta)$.

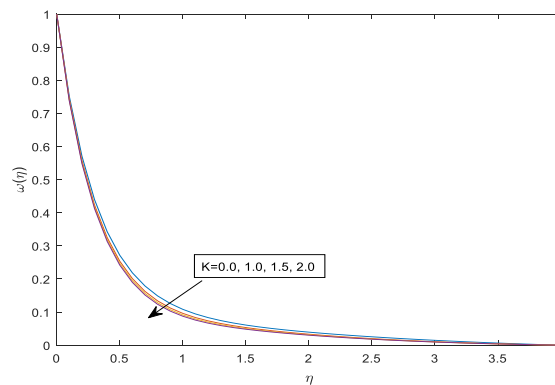


Figure 6. Effect of K on $\omega(\eta)$.

Figures 7–10 illustrate the impact of the chemical reaction parameter (Kc) on various profiles, specifically velocity, temperature, concentration, and the density of motile microorganisms. Figures 7, 9, and 10 collectively indicate a decrease in velocity, concentration,

and density profiles of motile microorganisms as Kc increases. However, Figure 8 reveals that the temperature of the fluid increases with the augmentation of Kc . The concentration profile exhibits a decreasing trend with respect to the parameter Kc . As the parameter Kc increases, the concentration profile diminishes.

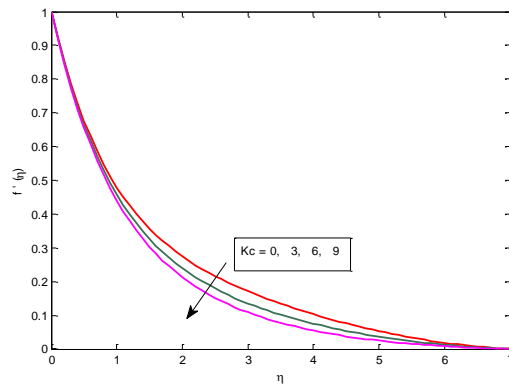


Figure 7. Effect of Kc on $f'(\eta)$

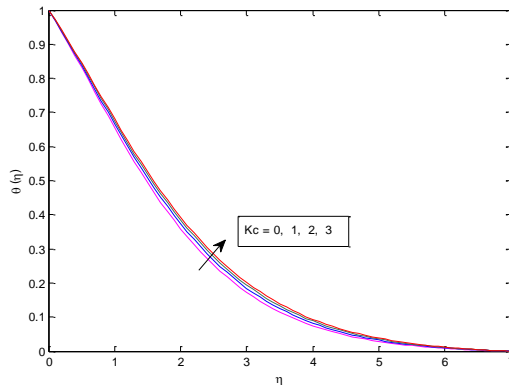


Figure 8. Effect of Kc on $\theta(\eta)$

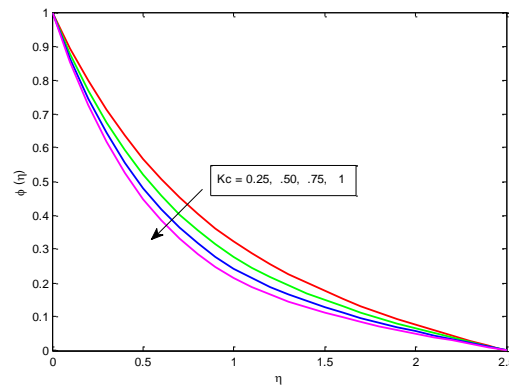


Figure 9. Effect of Kc on $\phi(\eta)$

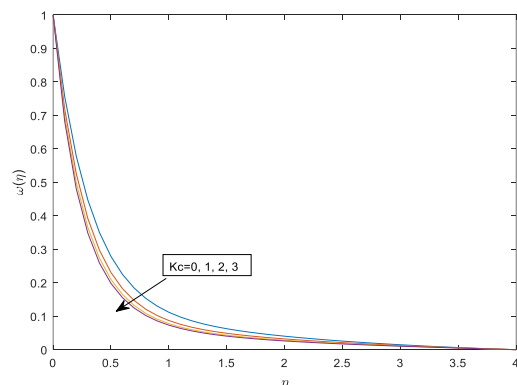


Figure 10. Effect of Kc on $\omega(\eta)$

Figures 11-13 show the influence of the Soret number (Sr) on the temperature, concentration, and density profile of the motile microorganisms. Figure 11 shows that the temperature of the fluid decreases with the Soret number. This observation suggests that increasing the Soret number (Sr) results in a reduction of the thermal boundary layer thickness. Figure 12 shows that the fluid concentration decreases with the Soret number. This means that the thickness of the concentration boundary layer decreases when the value of the Soret number is increased. Figure 13 shows that the density profile of the motile microbes increases with the Soret number.

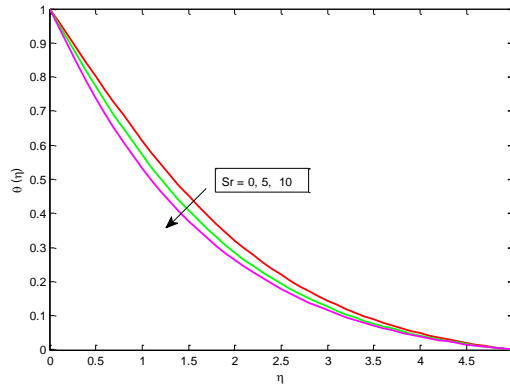


Figure 11. Effect of Sr on $\theta(\eta)$

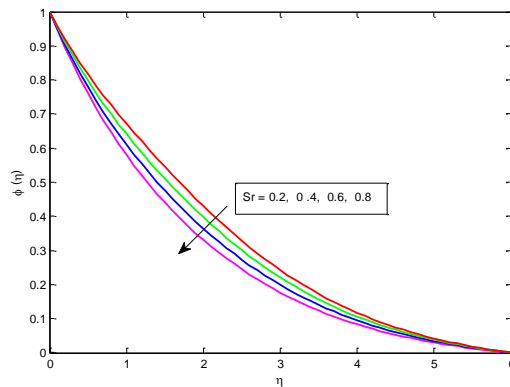


Figure 12. Effect of Sr on $\phi(\eta)$

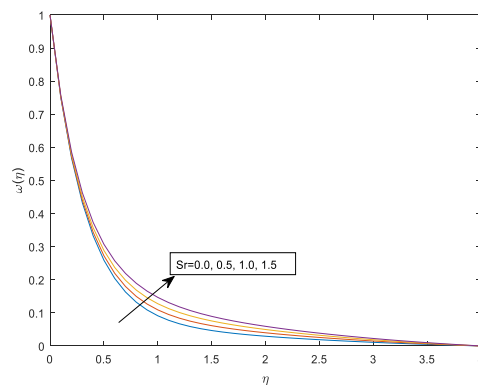


Figure 13. Effect of Sr on $\omega(\eta)$

Figures 14 and 15 depict the impact of Dufour number (Du) on the temperature profile and concentration profile, respectively. Figure 14 illustrates how the fluid's temperature increases as the Dufour number increases. This demonstrates that the thickness of the thermal boundary layer increases with the Dufour number. The fluid concentration decreases with the

Dufour number in Figure 15, indicating that a higher Dufour value results in a thinner concentration boundary layer.

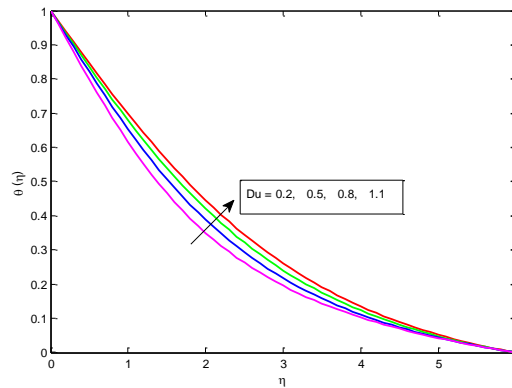


Figure 14. Effect of Du on $\theta(\eta)$

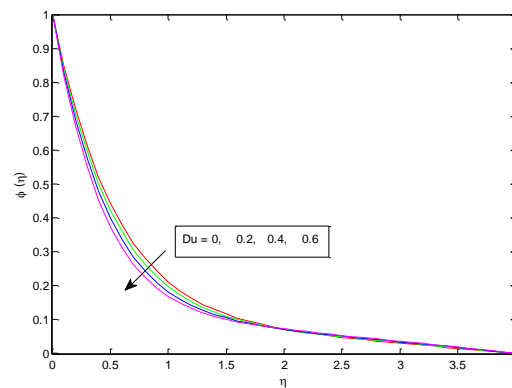


Figure 15. Effect of Du on $\phi(\eta)$

Figures 16-18 show the variation in the motile microbe density profile for different values of Sc_m , Pe and Le , respectively. From Figure 16, it is seen that there is a reduction in the motile microbe density profile with the rising values of Sc_m (Schmidt number for diffusing motile microorganisms). An elevation in the Sc_m notably diminishes the concentration contrast of microorganisms between the sheet and the region far from the sheet, resulting in a decline in the density profile of motile microorganisms. Figure 17 illustrates the motile microbe density profile for various values of Peclet number (Pe). The observation indicates that increasing Pe values lead to a decreasing trend in the distribution of motile microorganism density up to the region of $0 \leq \eta \leq 1.4$, after which a reverse effect is observed. Figure 18 demonstrates the impact of Le on the motile microorganism density profile. The results show that increasing the Lewis number (Le) decreases the diffusivity of microorganisms, which in turn reduces the density of motile microorganisms.

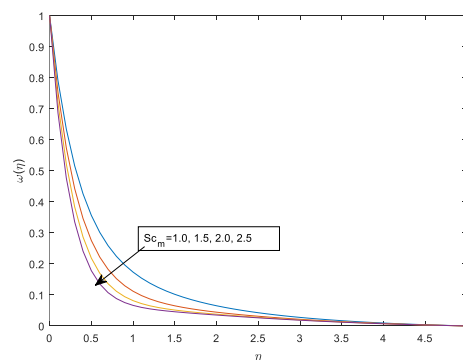


Figure 16. Effect of Sc_m on $\omega(\eta)$.

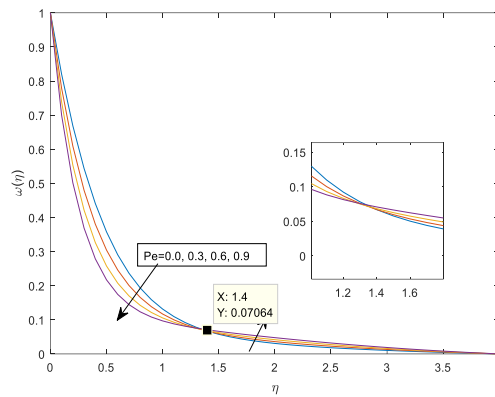


Figure 17. Effect of Pe on $\omega(\eta)$.

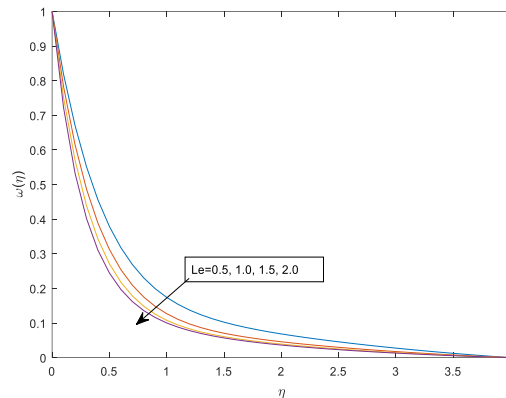


Figure 18. Effect of Le on $\omega(\eta)$.

Comparison of results for skin-friction coefficient and heat transfer rate in terms of Nusselt number with the previously published work by Rehman *et al.* [24] are shown in Table 1, and demonstrate favorable agreement between the findings.

Table 1. Comparison of $-f''(0)$ and $-\theta'(0)$ by varying M and Pr .

M	Pr	Rehman <i>et al.</i> [24]		Present study	
		$-f''(0)$	$-\theta'(0)$	$-f''(0)$	$-\theta'(0)$
0.0	0.71	1.0000130		1.0000089	
0.2		1.0954463		1.0954471	
0.5		1.2247454		1.2247456	
1.2		1.4832402		1.4832419	
2.0		1.7320516		1.7320523	
0.5	0.72		0.80875		0.80869
	1.0		1.00000		1.00000
	3.0		1.92375		1.92377

Finally, Table 2 presents the effects of the Soret number (Sr), chemical reaction parameter (Kc), and Dufour number (Du) on the skin friction coefficient (C_f), Nusselt number (Nu), and Sherwood number (Sh). The Nusselt number and the Sherwood number both increase as the Soret number (Sr) increases, whereas an opposite effect was observed for the skin friction coefficient. The Nusselt number is a physical quantity that indicates how much thermal convection contributes to heat conduction at the surface of the plate. The results indicate that enhancing the chemical reaction parameter (Kc) yields an increase in both the skin friction coefficient and the Sherwood number. However, the Nusselt number decreases with an increase in Kc . On the other hand, an increase in the Dufour number (Du) reduces both the skin friction coefficient and the Nusselt number. However, the Sherwood number increases as the Dufour number (Du) increases.

Table 2. Skin friction coefficient, Sherwood number, and Nusselt number values for a range Sr , Du and Kc values.

Sr	Du	Kc	C_f	Nu	Sh	
0.2	0.02	2	-1.58966	0.220841	0.987536	
0.4			-1.58889	0.221109	0.988597	
0.6			-1.58811	0.221378	0.989614	
1	0		-1.58694	0.229840	0.986780	
	0.4		-1.57921	0.053371	1.094556	
	0.8		-1.57122	-0.173970	1.239945	
	0.02		0	-1.55368	0.233080	0.471477
			1	-1.57656	0.225343	0.802901
			2	-1.58656	0.221917	0.991515

4. Conclusions

This study examines the combined effects of chemical reaction, Soret, and Dufour number on the flow of swimming gyrotactic microorganisms in micropolar nanofluid over a stretching/shrinking sheet with a heat source. In the presence of a uniform magnetic field, the research also considers the effects of buoyancy, viscous dissipation, and thermal radiation. The results show that the velocity and angular velocity profiles increase with the material parameter (K), while the temperature, concentration, and motile microorganisms density profile decreases with K . The chemical reaction parameter has a decreasing effect on velocity, concentration, and motile microorganism density profiles but an increasing effect on temperature profiles. The Soret number diminishes the temperature and concentration profiles, while the density profiles of the motile microorganisms increase with the Soret number. An increase in the Dufour number leads to a rise in fluid temperature but, conversely, decreases fluid concentration. The skin-friction coefficient rises with the chemical reaction parameter but decreases with the Soret and Dufour numbers. Increasing the Soret number enhances the heat transfer rate (Nusselt number), whereas increasing the Dufour number and chemical reaction parameter decreases it. Additionally, greater values of Sr, Du and Kc increase the mass transfer rate, as indicated by the Sherwood number. Also, the microorganisms' density profile decreases for increasing values of Le and Sc_m .

Funding

The present study has not been funded by any organization.

Acknowledgments

The authors are thankful to the anonymous reviewers for their insightful comments for improving the quality of the paper.

Conflicts of Interest

The authors declare no conflict of interest.

References

- Choi, S.U.; Eastman, J.A. Enhancing thermal conductivity of fluids with nanoparticles; Argonne National Lab.(ANL), Argonne, IL (United States): **1995**.
- Babu, D.V. Unsteady MHD free convection flow in a Casson Nano Fluid Through Porous Medium with Suction and Heat Source. *Int. J. Eng. Sci. Math.* **2019**, *8*, 62–75.

3. Xie, Z.; Jian, Y. Electrokinetic energy conversion of nanofluids in MHD-based microtube. *Energy* **2020**, *212*, <http://dx.doi.org/10.1016/j.energy.2020.118711>.
4. Ali, B.; Nie, Y.; Khan, S.A.; Sadiq, M.T.; Tariq, M. Finite Element Simulation of Multiple Slip Effects on MHD Unsteady Maxwell Nanofluid Flow over a Permeable Stretching Sheet with Radiation and Thermo-Diffusion in the Presence of Chemical Reaction. *Processes* **2019**, *7*, 628, <https://doi.org/10.3390/pr7090628>.
5. Mohyud-Din, S.T.; Khan, U.; Ahmed, N.; Rashidi, M.M. A study of heat and mass transfer on magnetohydrodynamic (MHD) flow of nanoparticles. *Propulsion and Power Research* **2018**, *7*, 72–77, <https://doi.org/10.1016/j.jprr.2018.02.001>.
6. Akbari, O.A.; Toghraie, D.; Karimipour, A.; Marzban, A.; Ahmadi, G.R. (2017) The effect of velocity and dimension of solid nanoparticles on heat transfer in non-Newtonian nanofluid. *Phys. Low-Dimensional Syst. Nanostruct* **2017**, *86*, 68–75, <https://doi.org/10.1016/j.physe.2016.10.013>.
7. Hayat, T.; Ahmad, S.; Khan, M. I.; Alsaedi, A. Simulation of ferromagnetic nanomaterial flow of Maxwell fluid. *Results in Physics* **2018**, *8*, 34–40, <https://doi.org/10.1016/j.rinp.2017.11.021>.
8. Kamal, F.; Zaimi, K.; Ishak, A.; Pop, I. Stability Analysis of MHD Stagnation-point Flow towards a Permeable Stretching/Shrinking Sheet in a Nanofluid with Chemical Reactions Effect. *Sains Malaysiana* **2019**, *48*, 243–250, <http://dx.doi.org/10.17576/jsm-2019-4801-28>.
9. Kumar, G.V.; Kumar, R.V.M.S.S.K.; Verma, S.V.K. Unsteady Magnetohydrodynamic Stagnation Point Flow of a Nanofluid over a Slendering Stretching Sheet Using Buongiorno's Model. *Int. J. Res. Ind. Eng* **2018**, *7*, 81–105, <http://dx.doi.org/10.22105/riej.2018.102367.1028>.
10. Mitra, A. Computational modelling of boundary-layer flow of a nano fluid over a convective heated inclined plate. *Journal of Mechanics of Continua and Mathematical Sciences* **2018**, *13*, 88–94, <http://dx.doi.org/10.26782/jmcms.2018.06.00006>.
11. Chakraborty, T.; Das, K.; Kundu, P.K. Ag-water nanofluid flow over an inclined porous plate embedded in a non-Darcy porous medium due to solar radiation. *J Mech. Sci. Technol.* **2017**, *31*, 2443–2449, <https://doi.org/10.1007/s12206-017-0442-4>.
12. Ziaei-Rad, M.; Kasaeipoor, A.; Lorenzini, G. A Similarity Solution for Mixed-Convection Boundary Layer Nanofluid Flow on an Inclined Permeable Surface. *Journal of Thermal Science and Engineering Applications* **2017**, *9*, 021015, <https://doi.org/10.1115/1.4035733>.
13. Raza, J.; Farooq, M.; Mebarek-Oudina, F.; Mahanthesh, B. Multiple Slip Effects on MHD non-Newtonian nanofluid flow over a nonlinear permeable elongated sheet: Numerical and statistical analysis. *Multidiscipline Modeling in Materials and Structures* **2019**, *15*, 913–931, <http://dx.doi.org/10.1108/MMMS-11-2018-0190>.
14. Mabood, F.; Shateyi, S. Multiple Slip Effects on MHD Unsteady Flow Heat and Mass Transfer Impinging on Permeable Stretching Sheet with Radiation. *Modelling and Simulation in Engineering* **2019**, 3052790, <https://doi.org/10.1155/2019/3052790>.
15. Das, U.J.; Dorjee, S. Magnetohydrodynamic Boundary Layer Flow with Soret/Dufour effects in presence of Heat source and Chemical Reaction. *Int. J. Appl. Eng. Res.* **2019**, *14*, 485–490.
16. Kumar, K.A.; Sugunamma, V.; Sandeep, N. Influence of viscous dissipation on MHD flow of micropolar fluid over a slendering stretching surface with modified heat flux model. *Journal of Thermal Analysis and Calorimetry* **2020**, *139*, 3661–3674, <http://dx.doi.org/10.1007/s10973-019-08694-8>.
17. Anwar, M.; Shafie, S.; Hayat, T.; Shehzad, S.A.; Salleh, M.Z. Numerical study for MHD stagnation-point flow of a micropolar nanofluid towards a stretching sheet. *J. Braz. Soc. Mech. Sci. Eng* **2017**, *39*, 89–100, <http://dx.doi.org/10.1007/s40430-016-0610-y>.
18. Kumar, K.A.; Sugunamma, V.; Sandeep, N. Thermophoresis and brownian motion effects on mhd micropolar nanofluid flow past a stretching surface with non-uniform heat source/sink. *Comput. Therm. Sci.: An Int. Journal* **2020**, *12*, 55–77, <http://dx.doi.org/10.1615/ComputThermalScien.2020027016>.
19. Kumar, K.A.; Sugunamma, V.; Sandeep, N.; Sivaiah, S. Physical aspects on mhd micropolar fluid flow past an exponentially stretching curved surface. *Defect and Diffusion Forum.* **2020**, *401*, 79–91, <http://dx.doi.org/10.4028/www.scientific.net/DDF.401.79>.
20. Venkata Ramudu, A.C.; Kumar, K.A.; Sugunamma, V.; Sandeep, N. Heat and mass transfer in mhd casson nanofluid flow past a stretching sheet with thermophoresis and brownian motion. *Heat Transfer* **2020**, *49*, 5020–5037, <http://dx.doi.org/10.1002/hjt.21865>.
21. Mabood, F.; Ibrahim, S.; Khan, W. Effect of melting and heat generation/absorption on siskonanofluid over a stretching surface with nonlinear radiation. *Phys. Scripta* **2019**, *94*, 065701, <https://doi.org/10.1088/1402-4896/ab1164>.

22. Sharada, K.; Shankar, B. MHD mixed convection flow of a Casson fluid over an exponentially stretching surface with the effects of Soret, Dufour, thermal radiation and chemical reaction. *World Journal of Mechanics* **2015**, *5*, 165–177, <http://dx.doi.org/10.4236/wjm.2015.59017>.
23. Abdal, S.; Ali, B.; Younas, S.; Ali, L.; Mariam, A. Thermo-Diffusion and Multislip Effects on MHD Mixed Convection Unsteady Flow of Micropolar Nanofluid over a Shrinking/Stretching Sheet with Radiation in the Presence of Heat Source, *Symmetry* **2020**, *12*, 49, <https://doi.org/10.3390/sym12010049>.
24. Rehman, S.; Mariam, A.; Ullah, A.; Asjad, M.I.; Bajuri, M.Y.; Pansera, B.A.; Ahmadian, A. Numerical computation of buoyancy and radiation effects on MHD micropolar nanofluid flow over a stretching/shrinking sheet with heat source. *Case Studies in Thermal Engineering* **2021**, *25*, 100867, <https://doi.org/10.1016/j.csite.2021.100867>.
25. Ramzan, M.; Chung, J. D.; Ullah, N. Radiative magnetohydrodynamic nanofluid flow due to gyrotactic microorganisms with chemical reaction and non-linear thermal radiation. *International Journal of Mechanical Sciences* **2017**, *130*, 31–40, <http://dx.doi.org/10.1016/j.ijmecsci.2017.06.009>.
26. Ahmad, S.; Younis, J.; Ali, K.; Rizwan, M.; Ashraf, M. *et.al.* Impact of Swimming Gyrotactic Microorganisms and Viscous Dissipation on Nanoparticles Flow through a Permeable Medium: A Numerical Assessment. *Journal of Nanomaterials* **2022**, 4888128, <https://doi.org/10.1155/2022/4888128>.
27. Hussain, A.; Malik, M. MHD nanofluid flow over stretching cylinder with convective boundary conditions and Nield conditions in the presence of gyrotactic swimming microorganism: A biomathematical model. *International Communications in Heat and Mass Transfer*, **2021**, *126*, 105425, <https://doi.org/10.1016/j.icheatmasstransfer.2021.105425>.
28. Shahid, A.; Zhou, Z.; Hassan, M.; Bhatti, M.M. Computational study of magnetized blood flow in the presence of Gyrotactic microorganisms propelled through a permeable capillary in a stretching motion. *Int J Multiscale Com.* **2018**, *16*, 303-320, <http://dx.doi.org/10.1615/IntJMultCompEng.2018026030>.
29. Waqas, H.; Khan, S.U.; Hassan, M.; Bhatti, M.M.; Imran, M. Analysis on the bioconvection flow of modified second-grade nanofluid containing gyrotactic microorganisms and nanoparticles. *J. Mol. Liq.* **2019**, *291*, 111231, <https://doi.org/10.1016/j.molliq.2019.111231>.
30. Koriko, O.K.; Omowaye, A.J.; Popoola, A.O.; Oreyeni, T.; Adegbite, A.A.; Oni, E.A.; Omokhuale, E.; Altine, M.M. Insight into Dynamics of Hydromagnetic Flow of Micropolar Fluid Containing Nanoparticles and Gyrotactic Microorganisms at Weak and Strong Concentrations of Microelements: Homotopy Analysis Method. *American Journal of Computational Mathematics* **2022**, *12*, 267-282, <https://doi.org/10.4236/ajcm.2022.122017>.